THESIS

EFFECT OF TREATMENT WITH A NRF2 ACTIVATOR ON IN VIVO PROTEOSTASIS IN MICE

Submitted by

Zackary J. Valenti

Department of Health and Exercise Science

In partial fulfillment of the requirements

For the Degree of Master of Science

Colorado State University

Fort Collins, Colorado

Summer 2019

Master's Committee:

Advisor: Karyn L Hamilton

Daniel S. Lark
Christopher L. Gentile

ABSTRACT

EFFECT OF TREATMENT WITH A NRF2 ACTIVATOR ON IN VIVO PROTEOSTASIS IN MICE

Aging is characterized by progressive declines in cellular function, often resulting from oxidative stress. Redox homeostasis is perturbed when the production of reactive oxygen species (ROS) exceeds the capacity of antioxidant defenses to eliminate ROS. Chronic imbalances in ROS production and clearance can lead to disruptions in proteostasis by causing unrepairable damage to proteins. Nuclear factor erythroid-derived 2-like 2 (Nrf2) exerts transcriptional regulation over endogenous antioxidant defenses by regulating the transcription of antioxidant enzymes and a myriad of cytoprotective proteins. Nrf2 activation has received attention as a therapeutic intervention to preserve cellular function. Our lab has characterized the treatment effects of Protandim and PB125, phytochemical compounds known to activate Nrf2. The collective findings from our group using both *in vitro* and *in vivo* experiments suggest that both compounds are effective for improving proteostasis; however, compared to Protandim, PB125 is more efficacious for sustained Nrf2 activation due to its ability to inhibit mechanisms of the Nrf2 shutdown pathway. We speculate that PB125 may have additional benefits on mechanism of proteostasis *in vivo*; thus, the purpose of the present study was to examine the effects of two doses of PB125 supplementation on proteostasis. We randomly assigned 51 male C57BL6/J mice aged 15-16 months to diets with 0 ppm (CON), 100 ppm (LOW), or 300 ppm (HIGH) doses of PB125

n=18/group during a 5-week feeding study. Mice were isotopically labeled with 8% deuterium oxide (D_2O) administered in the drinking water to simultaneously measure protein and DNA synthesis rates in mitochondrial (mito), cytosolic (cyto), and mixed (mixed) subcellular fractions of heart, liver, and skeletal muscle tissues. We hypothesized that mice treated with PB125 would have enhanced proteostasis outcomes; however, our results indicate that PB125 supplementation did not affect mechanisms of proteostasis. No significant differences were found in protein or DNA synthesis rates between treatment groups, and our secondary measures further support that PB125 did not affect the proteostatic network, as there were no significant differences observed in Nrf2-regulated protein expression or protein aggregation. From our data we were able to confirm that oral administration of PB125 is safe; however, further *in vivo* investigations are warranted in order to confirm the role of PB125 in modulating mechanisms of proteostasis.

TABLE OF CONTENTS

CHAPTER I: INTRODUCTION

I. Aging

Aging is the progressive decline in physiological function across the lifespan of an organism, which, at least in part, is attributable to accumulation of damage to proteins, lipids, and DNA (Richardson and Schadt 2014). Damage sustained to cellular structures over time is a consequence of chronic inflammation and excessive production of ROS (Murali and Panneerselvam 2007). ROS are inevitable by-products of life-sustaining metabolic processes (Richter-Dennerlein, Oeljeklaus et al. 2016). However, endogenous production of ROS becomes elevated with aging, effectively overwhelming the capacity of antioxidant defenses to maintain redox homeostasis (Seals, Jablonski et al. 2011). Accordingly, the aging phenotype is associated with high exposures to oxidative stress with consequent disruptions in proteostasis, or the maintenance of protein homeostasis (Klaips, Jayaraj et al. 2018). Moreover, a diminished capacity to maintain proteostasis induced by oxidative stress is central to the etiology of several age-related pathologies, including cardiovascular disease (McLendon and Robbins 2015), liver cirrhosis (Dasarathy and Hatzoglou 2018), and sarcopenia (Meng and Yu 2010).

Activation of the transcription factor Nrf2 induces the transcription of an array of genes encoding cytoprotective proteins that provide resistance to oxidative stress and inflammation, and promote maintenance of protein turnover (Nguyen, Nioi et al. 2009). Therefore, Nrf2 drives transcriptional regulation of redox-balance, inflammatory

processes, and mechanisms of proteostasis. While it has been reported that basal expression of Nrf2 is conserved in older animals, converging evidence suggests that Nrf2 activation and Nrf2-regulated protein expression is diminished during aging (Zhou, Zhang et al. 2018). Moreover, restoring the activity of Nrf2 through phytochemical activation is a promising therapeutic strategy, and Nrf2 activators are currently being investigated in clinical trials for their prospective beneficial effects on cellular function throughout lifespan.

II. Nrf2 Activators as Therapeutics

Protandim (LifeVantage, Corp.) and PB125 (Pathways Bioscience), commercially available plant derived phytochemical compounds known to activate Nrf2, have recently been pursued as a strategy for improving cellular function across the lifespan. Recent data from The National Institute on Aging Interventions Testing Program (ITP), a multi-institutional study designed to identify treatments with potential to extend lifespan and delay disease/dysfunction in mice, demonstrated that treatment with Protandim increased median lifespan of male HET3 mice (Strong, Miller et al. 2016). Additionally, our group has shown Protandim protects against oxidative stress induced cell death (Donovan, McCord et al. 2012, Reuland, Khademi et al. 2013). Although preliminary investigations with Protandim resulted in positive outcomes, the phytochemical cocktail PB125, a Nrf2 activator that results in more sustained activation of Nrf2 driven gene transcription, bears greater potential for lifespan extension compared to Protandim (unpublished data). Importantly, the active ingredients comprising PB125, carnosol,

luteolin, and withaferin A, have an extensive history of human consumption, and safety of these ingredients has been validated with both human and animal studies (AnadÓN, MartÍNez-LarraÑAga et al. 2008, Johnson 2011, Chandrasekhar, Kapoor et al. 2012). PB125 is currently being tested in the ITP, however, it is not yet clear if PB125 activates mechanisms responsible for protein homeostasis. Therefore, the purpose of the present study is to evaluate the effects of treatment with a potent Nrf2 activator, PB125, on rates of protein and DNA synthesis in male C57BL6/J mice.

III. Statement of the problem

The purpose of the present study is to examine the effects of treatment with PB125, a potent phytochemical Nrf2 activator, on rates of protein and DNA synthesis in heart, liver, and skeletal muscle in C57BL6/J mice aged 15-16 months over the course of a 5-week feeding study.

IV. Hypotheses

We hypothesize that mechanisms of proteostasis will be enhanced in subcellular fractions of heart, liver, and skeletal muscle of mice treated with PB125 compared to control.

CHAPTER II: LITERATURE REVIEW

I. Oxidative Stress

ROS are constantly formed during cellular metabolism, with endogenous sources of ROS being derived from electron leak during enzymatic reactions within the mitochondrial electron transport system. Briefly, complex I (NADH-CoQ reductase) and complex III (cytochrome C oxidase) are the primary production sites of the free radical superoxide anion ($O_2^{\bullet -}$) (Wong, Dighe et al. 2017). Superoxide anions have the potential to directly produce a more reactive radical, the hydroxyl radical (•OH) ($O_2^{\bullet -}$ + $2e^-$ → •OH). • OH is also produced indirectly through the dismutation of superoxide anion into hydrogen peroxide (H_2O_2) by the mitochondrial and cytosolic isoforms of the enzyme superoxide dismutase (SOD1/2) in conjunction with its metal co-factor Fe^{2+} (McCord and Fridovich 1968). Additional sources of ROS stem from peroxisomes (peroxidases, catalase, xanthine oxidase), lysosomes, and enzymes of the lipid bilayer (cyclooxygenases, lipoxygenases, and NADPH oxidases), producing a variety of ROS (Giustarini, Dalle-Donne et al. 2009).

Oxidative stress is characterized by a chronic imbalance in ROS production and a diminished capacity of antioxidant defenses to eliminate harmful reactive species, and it is theorized that oxidative stress-induced damage to macromolecular structures contribute to age-associated declines in cellular function (Beckman and Ames 1998). With advancing aging, endogenous antioxidant defenses become compromised and

lead to the accumulation of ROS (Okoduwa, Umar et al. 2015, Freitas, Boncompagni et al. 2016). The data currently available suggest that ROS-induced lipid and protein modifications such as peroxidation, carbonylation, nitrosylation and glycation are linked to the progression of age-related diseases like cardiovascular disease, liver cirrhosis, and sarcopenia. For example, older individuals afflicted by vascular endothelial dysfunction possess elevated levels of nitrotyrosine, whereas liver cirrhosis patients have increased oxidatively modified lipids (ie. lipid peroxidation) that are associated with ROS accumulation (Donato, Eskurza et al. 2007, Reynaert, Gopal et al. 2016). The plasma of sarcopenic individuals compared to their non-sarcopenic counterparts have higher levels of 4-hydroxynonenal (4-HNE), a modified protein end-product resulting from ROS exposure (Bellanti, Romano et al. 2018). It has become apparent that high exposure to ROS contributes to the etiology of age-related diseases and causes disruptions in redox signaling, likely due to a decreased capacity to eliminate harmful ROS (Bakala, Delaval et al. 2003). However, low exposure to oxidants is essential for healthy redox signaling and, further, to promote adaptive cellular responses that are coordinated by the Nrf2-Keap1-ARE axis (Tebay, Robertson et al. 2015, Egea, Fabregat et al. 2017) .

II. Nrf2-Keap1-ARE Axis

Under normal physiological conditions Nrf2 resides in the cytosol bound to Kelch-like ECH-associated protein 1 (Keap1), a cytoskeleton-associated adaptor protein that negatively regulates Nrf2 activity (Zhang, Lo et al. 2004). Keap1 serves as a redox

sensor of the cellular environment, responding to the presence of Nrf2 activators such as oxidants, electrophiles, xenobiotics, and phytochemicals (Wu, McDonald et al. 2014). Nrf2 activators interact with key cysteine thiol residues of Keap1, enabling Nrf2 to be released from Keap1 and translocate to the nucleus. Once inside the nucleus, Nrf2 is able to interact with the Antioxidant/Electrophilic Response Element (ARE), a transcriptional element responsible for regulation of gene targets involved in redox regulation, phase I-III drug metabolism, iron and heme metabolism, autophagy, and proteasome assembly (Dodson, de la Vega et al. 2019).

Nrf2 activity is repressed by Keap1, which is comprised of several domains that collectively regulate Nrf2. The double-glycine repeat region (DGR) of dimerized Keap1 binds the Neh2 domain of Nrf2, driving the formation of Nrf2-Keap1 complex in a “hinge-and-latch” mechanism. As a result, Nrf2 is kept sequestered in the cytosol by Keap1, preventing its nuclear translocation (Itoh, Wakabayashi et al. 1999). It is important to note that in non-stressful conditions, Keap1 promotes the degradation of Nrf2 by the ubiquitin proteasomal system (UPS). The process of Nrf2 degradation occurs at the intervening region (IVR) of Keap1, which recruits RING-box-protein 1 (Rbx1) and binds Cullin-3 (Cul3), an E3-ubiquitin ligase that is necessary for Nrf2 ubiquitination and subsequent degradation by the 26s proteasome (Zhang, Lo et al. 2004). This degradatory mechanism serves as a primary regulator of Nrf2 activity. The IVR is a cysteine-rich domain that is sensitive to oxidative modification, primarily by RONS or electrophilic stress (Canning, Sorrell et al. 2015). Moreover, molecular interactions

between Nrf2 and Keap1 allows for the rapid detection of changes to redox homeostasis in the cytosol and drives gene transcription through the Nrf2-ARE axis.

III. *Nrf2 Activation and Gene Targets of the ARE*

Under conditions of oxidative stress, cysteine residues within Keap1 are oxidized causing a conformational change in the Nrf2-Keap1 complex that effectively stabilizes Nrf2. Lysine residues on Nrf2 become hidden and can no longer be ubiquitinated, preventing Nrf2's degradation and increasing its half-life from roughly 15 to 180 minutes (Lewis, Mele et al. 2010). Subsequently, Nrf2 can translocate to the nucleus. Nuclear accumulation of Nrf2 results in the formation of heterodimers with small masculoaponeurotic fibrosarcoma (MAF) proteins and facilitates binding of Nrf2 to the cis promoter region of the ARE. The Nrf2-ARE interaction induces expression of a myriad of cytoprotective genes that maintain redox homeostasis. (MacLeod, McMahon et al. 2009).

Activation of Nrf2 has been identified as a novel therapeutic strategy primarily because of its ability to induce the expression of antioxidant transcriptional programs. An important function of Nrf2-related antioxidants is to maintain redox homeostasis via adequate regulation of proteins involved in glutathione metabolism (Chen, Liu et al. 2010). Accordingly, GSH levels are regulated by Nrf2 gene targets GCLM and GCLC, which encode for glutamate cysteine ligase, the protein responsible for de novo biosynthesis of GSH (Wild, Moinova et al. 1999) Also requisite for GSH synthesis is the

cysteine importer xCT, encoded by the Nrf2 gene target SLC7A11. Nrf2 activation was shown to induce expression of xCT mRNA that preceded any increase in GSH protein levels (Nishimoto, Koike et al. 2017). With regard to GSH and Nrf2, GPX2 and GPX4 are gene targets of Nrf2 encoding glutathione peroxidases, which reduce peroxides by using GSH as a substrate (Friedmann Angeli, Schneider et al. 2014). Another important antioxidant protein downstream of Nrf2 is glutathione reductase (GR), which catalyzes the reduction of oxidized glutathione (GSSG) back to GSH. Serving as a crucial redox buffer, GSH is present in high concentrations in the cytosol, nucleus, and mitochondria (Valko, Leibfritz et al. 2007). The ratio of reduced to oxidized glutathione (GSH:GSSG) is an indicator of cellular redox status, and is both directly and indirectly affected by Nrf2 driven expression of antioxidants. In summary, Nrf2 maintains cellular redox homeostasis by inducing gene expression of antioxidant proteins via the ARE.

The transcription factor Nrf2 is also implicated in drug and xenobiotic metabolism. The most extensively studied proteins are involved in phase I and II metabolism, which reduce toxins and drugs into harmless metabolites. Nrf2 drives expression of aldo-keto reductases, aldehyde reductases, and NAD(P)H:quinone oxidoreductase 1 (NQO1), another enzyme key to antioxidant defenses (Itoh, Chiba et al. 1997). NQO1 effectively combats oxidative stress by detoxifying quinones and preventing redox cycling, a series of reactions that propagate free radical production (Gaikwad, Long et al. 2001). Lastly, Nrf2 has also been reported to enhance the transcription of a class of membrane transporters of the ATP-binding cassette family, functioning to excrete xenobiotics/drugs from the cell (Wu, Cui et al. 2012). Nrf2 knockout mice are highly sensitive to

acetaminophen-induced hepatotoxicity, and this was associated with reduced expression of Nrf2-regulated drug metabolizing enzymes and antioxidants (Enomoto 2001). To recapitulate, Nrf2 transcriptionally regulates the expression of a functionally diverse set cytoprotective proteins.

IV. *Nrf2 & Proteostasis*

Activation of Nrf2-ARE driven gene transcription has been identified as a modulator of proteostasis, as Nrf2 coordinates gene transcription of cytoprotective proteins that provide resistance to oxidative stress and assuage disruptions in proteostasis. Maintaining the proteostatic network requires a functional equilibrium between protein synthesis, folding, localization and degradation processes (Diaz-Villanueva, Diaz-Molina et al. 2015). Protein turnover, the balance between protein synthesis and degradation processes, is essential for protein homeostasis. Sustaining adequate rates of protein turnover reduces the potential for damage to macromolecular structures. This is important because the enzymatic capacity to repair damaged proteins is limited and declines further with age, requiring damaged and/or dysfunctional proteins to be degraded to their amino acid constituents (Ryazanov and Nefsky 2002). In concordance with this idea, loss of proteostasis has emerged as a hallmark of the aging process, with the current body of literature suggesting that the capacity to maintain proteostasis declines over lifespan (Basisty, Meyer et al. 2018). While insufficient protein turnover is one manifestation, loss of proteostasis is also characterized by altered post-translational modifications, protein aggregation, oxidative damage, and misfolding events at the

cellular level. Furthermore, new protein synthesis contributes to establishing a functionally stable proteome in the cell and is a cornerstone of maintaining cellular function.

Nrf2 signaling may serve as a promoter of protein turnover due to its role in regulating the proteasome and autophagy, two critical mechanisms facilitating protein degradation. Briefly, the proteasome works in conjunction with the ubiquitin system to degrade short-lived regulatory proteins and misfolded proteins (Diaz-Villanueva, Diaz-Molina et al. 2015), and proteasomal assembly requires the expression of proteasome subunit α1 (PSMA1), proteasome subunit β5 (PSMB5), and proteasome maturation protein (POMP), which all contain ARE sequences and are transactivated by Nrf2 (Kwak, Wakabayashi et al. 2003, Jang, Wang et al. 2014). Distinct from proteasomal degradation is autophagy, a process that eliminates protein aggregates, as well as organelles such as the mitochondria and endoplasmic reticulum (Noda and Inagaki 2015). At the juxtaposition of autophagy and Nrf2 signaling is p62/sequestosome1 (p62), an adaptor protein that binds ubiquitinated proteins and delivers cargo to the autophagosome during autophagic clearance (Lim, Lachenmayer et al. 2015, Liu, Ye et al. 2016). p62 links autophagy to the Nrf2-Keap1-ARE axis through its interaction with Keap1, as p62 contains a binding motif similar in structure to Nrf2, allowing it to interact directly with Keap1 and initiate its degradation (Liu, Ye et al. 2016). Phosphorylation of p62 at serine351 increases its binding affinity for Keap1, causing Nrf2's dissociation and subsequent nuclear accumulation (Komatsu, Kurokawa et al. 2010). Interestingly, p62 expression is upregulated in response to Nrf2 activation, creating a positive feedback

loop that promotes Nrf2 activity through the autophagic clearance of Keap1 (Jain, Lamark et al. 2010). Investigations using p62 KO mice have revealed that p62 is necessary for the expression of NQO1 in oxidative skeletal muscle, indicating that p62 cooperates with Nrf2 to induce antioxidant expression (Yamada, Iwata et al. 2019). Pertaining to Nrf2's role in activating transcriptional programs of autophagic machinery, autophagy related proteins 5 and 7 (ATG) and unc-51-like autophagy activating kinase 1 and 2 (ULK1/2), are encoded by autophagy genes containing an ARE sequence (Pajares, Jiménez-Moreno et al. 2016). Intuitively, these genes are inducible by Nrf2 activation, placing Nrf2 in a governing role over mechanisms of protein degradation.

Nrf2 functions to coordinate an adaptive response to stressors, contributing to the maintenance of protein homeostasis. Importantly, Nrf2 preserves endoplasmic reticulum (ER) function by participating in the unfolded protein response (UPR) in concert with protein kinase R-like endoplasmic reticulum kinase (PERK) (Cullinan and Diehl 2006, Xie, Pariollaud et al. 2015). The ER is considered a key component of the proteostasis network, as the ER is the main site of ribosomal translation and post-translational folding of proteins. Localized to the ER membrane, PERK is a transdomain kinase that mediates signal transduction from the ER lumen to the cytosol and nucleus (Harding, Zhang et al. 1999). The ER possesses sensors, like that of PERK, that detect the accumulation of unfolded/misfolded proteins and stimulate various effectors to prevent proteotoxicity and cell death. Specifically, unfolded proteins unveil hydrophobic residues that are recognized by BIP, a chaperone that is released from PERK's lumenal domain upon activation by proteotoxic stress (Kohno, Normington et al. 1993).

Simultaneously, PERK activation results in the direct phosphorylation of serine residues on eukaryotic initiation factor-alpha (eIF2α) and Nrf2, exerting regulation over protein synthesis and progression through the cell cycle in response to stress (Ron and Walter 2007, Chevet, Hetz et al. 2015).

UPR-activated PERK signaling functions to repress global protein translation at the onset of ER stress (Cullinan and Diehl 2004). Initiation of the UPR stimulates PERK to phosphorylate the translation initiation factor eIF2α, causing the inhibition of translation initiation (Harding, Zhang et al. 2000). Perturbations in ER homeostasis additionally provoke PERK-dependent phosphorylation of Nrf2, causing Nrf2 to be released from Keap1 and translocate to the nucleus (Cullinan, Zhang et al. 2003). In agreement with this idea, the early stages of oxidative stress promote the PERK-Nrf2 signaling pathway to arrest cell cycle via modification of cyclin activity and concentration. Cell cycle progression is intricately regulated by a complex network of cyclin dependent kinases and their respective cyclin substrates (Malumbres 2014), and are further influenced by PERK signaling. At the initial stage of mild oxidative stress, Nrf2 prompts cell cycle arrest in G2 by binding to the genetic promoters of p15, p17, and p21, the putative stochiometric inhibitors of cyclin D1 activity (Márton, Tihanyi et al. 2018). In contrast, prolonged exposure to oxidative stress initiates the degradation of Cyclin D1 in a PERK-dependent manner, resulting in decreased cyclin D1 protein concentration (Márton, Tihanyi et al. 2018). To summarize, the PERK-Nrf2 signaling pathway is an adaptive response to oxidative stress that serves to block cell cycle progression by controlling cyclin D1 activity and concentration (Harding, Novoa et al. 2000).

In parallel with the aforementioned responses to oxidative stress, cells possess additional control mechanisms that modulate cell cycle to promote cell survival. p53, a transcription factor that ensures genome integrity by organizing responses to DNA damage, is central to the counteraction of oxidative stress (Hiemstra, Niemeijer et al. 2017). Conditions of prolonged exposure to high concentrations of ROS causes oxidation of redox-sensitive cysteines within p53, leading to the expression of gene targets that collectively prompt DNA repair, cell cycle arrest, and apoptosis (Fischer, Prodeus et al. 2016). Activation of p53 has been identified as a regulator of Nrf2 activity, eliciting a diphasic response that is dependent on the degree of oxidative stress (Chen, Jiang et al. 2012). On one hand, mild conditions of oxidative stress are associated with low levels of p53 and transcriptional activation of p21, a cyclin dependent kinase inhibitor that arrests cell cycle at G1 (Cao, Li et al. 2013). The p53-dependent block in cell cycle progression allows for the immediate upregulation of Nrf2-dependent antioxidant gene transcription, restoration of redox-balance, and subsequent cell cycle re-entry. However, when cells are subjected to conditions that invoke cellular damage, p53 becomes elevated and the Nrf2 response is suppressed (Chen, Jiang et al. 2012). Simultaneous to the suppression of Nrf2-dependent antioxidant response, p53 initiates apoptosis, a cell death process that preserves the genome (Luo, Liang et al. 2017). In review, p53 regulates Nrf2 to counteract the consequences of ROS accumulation in a spatiotemporal manner, as mild concentrations of ROS activates p53 and bolsters the strength of Nrf2-dependent antioxidant scavenging, while unrepairable cellular damage

induced by excessive ROS causes p53 to block cell cycle progression and induce apoptotic cell death (Faraonio, Vergara et al. 2006).

The diversity of Nrf2's interactions with the proteostatic network lends significance to the central role of Nrf2 in mediating cellular function. Nrf2 is vital for not only the immediate restoration of redox-balance, but also the regulation of protein synthesis and degradation, the UPR, and several aspects of the cell cycle. With the convoluted nature of Nrf2 signaling, investigating the role of Nrf2 in the context of proteostasis requires consideration of both protein and DNA synthesis. Accordingly, the present study assessed the contribution of new protein synthesis and cellular proliferation to proteostasis by measuring rates of protein and DNA synthesis.

CHAPTER III: METHODS

I. Animal Care

51 male C57BL/6J mice aged 15-16 months were purchased from Jackson Laboratories. All animals were housed at the Painter Center, home of Colorado State University's (CSU) Laboratory Animal Resources facilities. All procedures were approved by the CSU Animal Care and Use Committee, and met or exceeded animal housing standards as described in the Animal Welfare Act regulations, the Guide for the Care and Use of Laboratory Animals, and the Guide for Care and Use of Agricultural Animals in Agricultural Research and Teaching.

II. Diet Composition – PB125 (Pathways Bioscience)

Diets were supplemented with PB125, consisting of a combination of three plant-derived phytochemicals [*Carnosol* (Rosemary extract), *Withaferin A* (Ashwaganda), and *Luteolin*) at two doses in pellet form (Dyets Inc, Bethlehem, PA). The dietary composition for each dose is listed as follows: The low dose (100 ppm) dietary supplement consisted of Rosemary extract (6.82×10^{-6} mg/g diet), Withaferin A (2.27×10^{-5} mg/g diet), Luteolin (9.09×10^{-6} mg/g diet). The high dose (300 ppm) consisted of Rosemary extract (2.05×10^{-4} mg/g diet), Ashwaganda extract (1% withaferin A)(6.82×10^{-5} mg/g diet), Luteolin (2.73×10^{-5} mg/g diet).

III. Experimental Design

Mice were randomly assigned to one of three diet groups (n=18/group), consuming either CON, LOW, or HIGH doses of PB125 (Figure 1). PB125 was provided ad-libitum for the 5-week duration of the study. Mouse body weights and food intake were recorded at baseline, then recorded every other day until the completion of the 5-week feeding period. Collected data were averaged to obtain mean body weight (Luo, Liang et al.) and mean daily food intake (Luo, Liang et al.).

IV. Deuterium Labeling

Following a 7-day lead-in on the diet, mice were isotopically labeled with deuterium oxide (D_2O) to measure protein and DNA synthesis (Figure 1). Mice received a bolus intraperitoneal (i.p) injection of 99% D_2O (Sigma-Aldrich, St. Louis, MO, USA) in 0.9% NaCl relative to 60% of body weight as previously described (Drake, Bruns et al. 2014) and 8% D_2O was added to the drinking water for the duration of the feeding period to maintain D_2O enrichment. D_2O incorporates into non-labile sites on alanine and deoxyribose, providing a strategy to determine fractional synthesis rates (FSR) of protein and DNA.

V. Animal Sacrifice & Tissue Harvest

12 hours prior to sacrifice, all food was removed from each cage to illicit an overnight fast. All animals were anesthetized via i.p. injection with 0.5-1.0 mL of ketamine (80mg/kg)/xylazine (20mg/kg) solution. Takedowns were performed at 1, 4, 8, 14, and 34 days of deuterium labeling (n=3-4 mice/group/day) and tissues were harvested to

capture protein and DNA synthesis for the full duration of the labeling period (Figure 1). Blood was obtained by cardiac venipuncture (approx. 1.0mL), immediately followed by excision of heart, liver, and gastrocnemius, and bone marrow was extracted from the tibia and femur. All tissues were rinsed in phosphate buffered solution (PBS), dissected of connective tissue and weighed on an analytical balance (Denver Instruments) accurate within ± 0.1g. Tissues were then flash frozen in liquid nitrogen and stored at -80°C for future analysis.

VI. Tissue and Analyte Preparation

a. Body Water Derivation and Analysis

Body water deuterium enrichment was determined from plasma as previously described by our lab (Miller, Robinson et al. 2012). Plasma was obtained by centrifugation of 1.0 ml blood samples at the time of sacrifice. 125 uL of plasma was pipetted into the inner well of an o-ring screw cap, and tubes were inverted and incubated on a heat block overnight at 80°C. Following overnight incubation, samples were cooled to room temperature and 2 uL of 10M NaOH and 20 mL of acetone were added to each sample and 0%-20% D_2O standards. Samples were then briefly vortexed and allowed to incubate overnight at room temperature. The following day, all samples and standards were prepared for acetone derivation and subsequent extraction by adding 200 uL of hexanes. The organic layer was transferred to gas-chromatography vials with 200 uL pipette tips containing Na_2SO_4. Samples were analyzed via gas-chromatography/mass-spectrometry on EI Mode with a DB-17MS column. The mass-to-charge ratios of 58 and

60 were monitored for the acetone derivative and quantified using ChemStation software (Agilent Technologies, Santa Clara, CA, USA).

b. Tissue Fractionation by Differential Centrifugation

Approximately 40-50 mg of whole skeletal muscle, heart, and liver tissue samples were pulverized under liquid nitrogen and used for differential centrifugation to isolate mitochondrial enriched (mito), cytosolic (cyto), and mixed (mixed) subcellular protein fractions according to our previously published procedures (Miller, Robinson et al. 2013, Drake, Bruns et al. 2014). Pulverized tissues were bead homogenized in 1:10 isolation buffer (100 mM KCl, 40 mM Tris HCl, 10 mM Tris Base, 5 mM $MgCl_2$, 1 mM EDTA, 1 mM ATP, pH 7.5) with addition of phosphatase and protease inhibitors (HALT, Thermo Scientific, Rockford IL). The initial tissue homogenate was centrifuged at 800g for 10 min at 4°C. The resulting supernatant was removed and added to a new tube, and the pellet was saved as mixed. The supernatant from the previous spin was centrifuged at 10,000g for 30 min at 4°C, and the resulting pellet was saved as mito. From the supernatant, 400 uL was removed and an equal volume (400 uL) of 14% SSA was added. The tube incubated on ice for 1hr and labeled as cyto. The remaining volume of supernatant from the mito spin was saved for protein quantification. The mito pellet was washed with 200 uL buffer #2 (100 mM KCl, 10 mM Tris-HCl, 10 mM Tris Base, 1 mM $MgSO_4$, 0.1 mM EDTA, 0.02 mM ATP, and 1.5% BSA, pH 7.4) and centrifuged at 8000g for 10 min at 4°C. The supernatant was removed, and the pellet was washed a second time with 100uL buffer #2 and centrifuged at 6000g for 10 min at 4°C. Following the 6000g spin a final wash step with 1ml ddH_2O was performed. After the 1 hr

incubation, the cyto tube was centrifuged at 16,000g for 10 min at 4°C to yield the Cyto protein pellet. The cyto and mixed pellet were washed with 500 uL 100% ethanol, centrifuged at 1000g for 4 min at 4°C, and washed with 500 uL ddH_2O and centrifuged again at 1000g for 4min at 4°C. cyto and Mix wash steps were repeated once. mito, cyto, and mixed pellets were solubilized in 250 uL 1M NaOH for 15 min at 50°C and hydrolyzed in 6M HCl for 24 hours at 120°C.

c. Alanine Derivation and Analysis

Protein was hydrolyzed overnight in 6M HCl at 120°C. Protein hydrolysates were cation exchanged and dried under vacuum according to our previous published procedures (Miller, Robinson et al. 2012) Dried hydrolysates were resuspended in 1 mL of molecular biology grade water, and approximately 500 uL of sample was used for derivation. 500 uL acetonitrile, 50 uL1M K2HPO4, and 20 uL of pentafluorobenzyl bromide were added to all samples and standards. Tubes were vortexed and incubated on a heating block at 100°C for 1 hour. Samples were removed from the heating block and cooled to room temperature. Once cooled, 600 uL of ethyl acetate was added to each sample and vortexed vigorously to allow for phase separation. Using a Pasteur pipette, the organic layer was transferred to GC vials and dried down under N_2. After drying, samples were reconstituted in 700 uL ethyl acetate, vortexed, and tightly capped for analysis on GC/MS. Samples were analyzed by negative chemical ionization in selective ion monitoring mode. A DB225 gas chromatograph column was used to separate amino acid derivatives. Starting temperature was 100°C and increased to 220°C at a rate of 10°C per minute with helium as the carrier gas and methane as the reagent. The mass-to-charge ratios of 448, 449, and 450 were monitored for the

pentafluorobenzyl-*N*,*N*-di(pentafluorobenzyl)alaninate derivative, and quantified using ChemStation software (Agilent Technologies, Santa Clara, CA, USA). The mass-to-charge ratios represented the primary daughter ions that included all of the original hydrocarbon bonds from the given amino acid. ^{2}H enrichment was calculated as the M+1 mass isotopomer divided by the sum of the M+1 and M+0 mass isotopomers (Hellerstein & Neese, 1999). The newly synthesized fraction of proteins was calculated by dividing the deuterium enrichment of alanine from protein by the precursor enrichment from body water (plasma). The precursor enrichment was determined from the enrichment of deuterium in body water and adjusted using mass isotopomer distribution analysis (MIDA) to determine alanine enrichment (Hellerstein & Neese, 1999). Protein synthetic rates were calculated by dividing fraction new by time and expressed as fractional synthesis rates (%FSR/day).

d. DNA Extraction and Derivation

DNA was isolated from whole tissue and bone marrow (QIAamp DNA mini kit, Qiagen, Valencia, CA, USA) and hydrolyzed overnight at 37°C with nuclease S1 and potato acid phosphatase. Next, 80uL of glacial acetic acid and 100 uL pentafluorobenzyl hydroxylamine solution were added to sample hydrolysates and standards (1-30 ug/ml range deoxyribose) and incubated on a heating block for 30 min at 100°C. Following incubation, samples were cooled to room temperature and then reacted with 1ml acetic anhydride and 100 uL n-methylimidazole for 15-20 minutes. After the reaction reached completion, 2ml molecular biology grade water and 750uL methylene chloride were

added to each tube and vortexed to induce phase separation. The bottom organic layer was extracted and expelled into a new tube containing granular anhydrous Na_2SO_4. An additional 750uL methylene chloride was added to samples, and extraction steps were repeated. Extraction was then transferred from tubes containing Na_2SO_4 to GC vials. GC vials were vacuum dried for one hour and reconstituted in 70uL ethyl acetate. Ethyl acetate was transferred to tapered GC vial insert and placed back into GC vials, which were tightly capped for GC/MS analysis. Samples were then analyzed by GC/MS with a DB-17MS column using negative chemical ionization with helium as the carrier gas and methane as the reagent. The pentafluorobenzyl triacetyl derivative of purine dR was monitored for the fractional molar isotope abundances at m/z 435 and 436, and quantified using ChemStation software (Agilent Technologies, Santa Clara, CA, USA). DNA fraction new was calculated in comparison to bone marrow, which represents a fully turned over population of cells (Miller et al., 2012). DNA synthesis rates were calculated by dividing DNA fraction new by time and expressed as fractional synthesis rates (FSR%/day). The protein FSR was then expressed relative to the DNA FSR to obtain the PRO:DNA synthesis ratio.

VII. Immunoblotting & Band Detection

Heart, liver, and skeletal muscle were homogenized using lysis buffer composed of 50 mM HEPES, 12 mM Na4P207, 100 mM NaF, 10 mM EDTA, 400μL of Protease and Phosphatase Inhibitors, and 5 mL of 10%Triton. Protein (30 μg) was loaded onto a 8-16% SDS-PAGE gel, run at 200V for one hour and transferred to PVDF membranes. Membranes were then probed with the primary antibodies glutathione-S-transferase

(Abcam-ab180650), thioredoxin reductase 1 (Novus-6925S), and glutathione reductase (Abcam-16801) diluted to 1μg/mL and placed on a plate shaker overnight at 4°C. After washing with TBST, the membranes were incubated with horse-radish peroxidase-conjugated anti-rabbit secondary antibodies (Cell Signaling-7074P2) and TBST washing was repeated. Protein bands were imaged on a FluorChem E chemiluminescence imager (Protein Simple) and quantified using AlphaView SA software.

VIII. Protein Aggregation

Skeletal muscle and liver protein aggregation were determined using the Proteostat protein aggregation assay, fluorescence-based assay kit (Enzo Life Sciences). Protein was added to 1X diluted Proteostat assay buffer. Once in solution, 98 µL of protein (10*µ*g/mL) was loaded onto a 96-well plate with 2 µL of 1X diluted Proteostat detection reagent, then incubated in the dark at room temperature for 15 minutes. The microplate was then read with a fluorescence microplate reader at an excitation setting of 550 nm and an emission filter of 600 nm. The resulting signal was compared against a standard curve of aggregated IgG generated from Proteostat standards and normalized to total protein.

IX. Statistics and Data Analyses

Statistical analyses were performed using Prism Graphpad Version 8 (La Jolla, CA). All values are presented as means ± SEM. Changes in protein turnover over time were determined by a two-way ANOVA as treatment by time, while individual time points (protein synthesis, western blots, and protein aggregation) were analyzed using a one-way ANOVA. Statistical significance was set a priori at $P < 0.05$.

CHAPTER IV: RESULTS

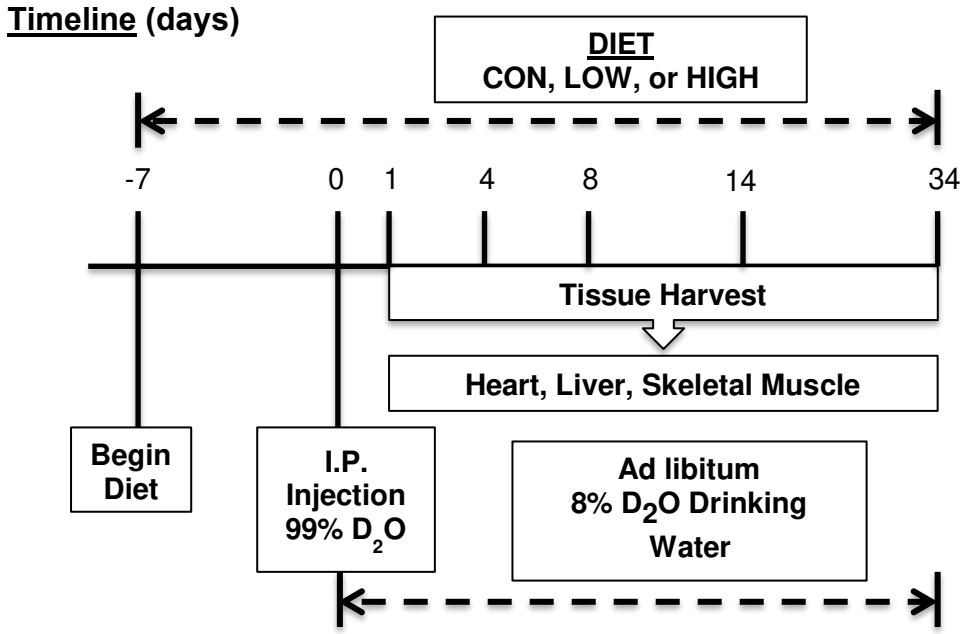

Figure 1. Timeline of experimental design. Mice received a bolus interperitoneal injection of 99% D_2O following a week lead in on either CON, LOW, or HIGH PB125 supplemented diets. 8% D_2O was supplied to the mice ad-libitum for the duration of the feeding period to maintain the enrichment of D_2O in the body water. Mice were sacrificed and tissues were harvested after 1, 4, 8, 14, and 34 days of deuterium labeling (n=3-4 mice/treatment group/time point)

A

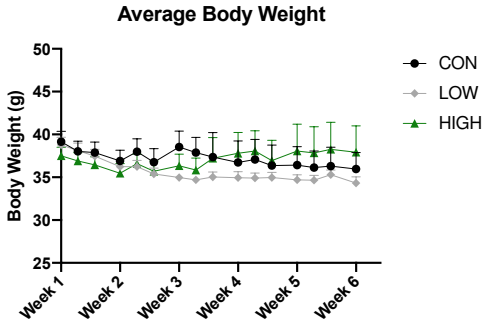

B

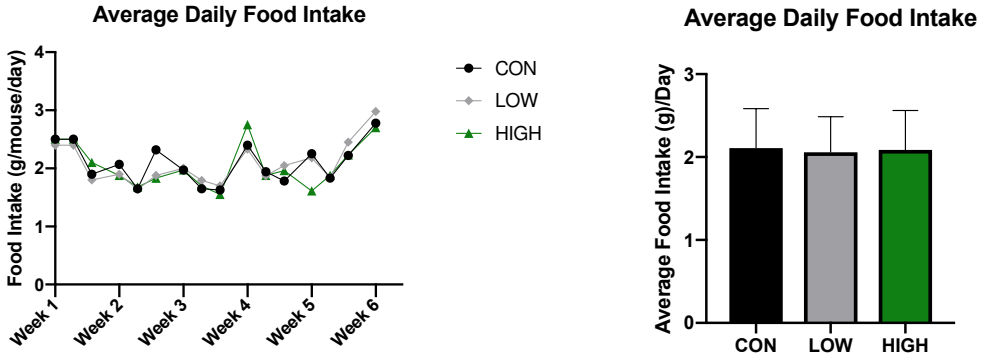

Figure 2. Average body weight (g) (A). Average daily food intake (g)/day (B) for mice treated with CON, LOW, or HIGH doses of PB125. * denotes significant difference from pre (P < .0001)

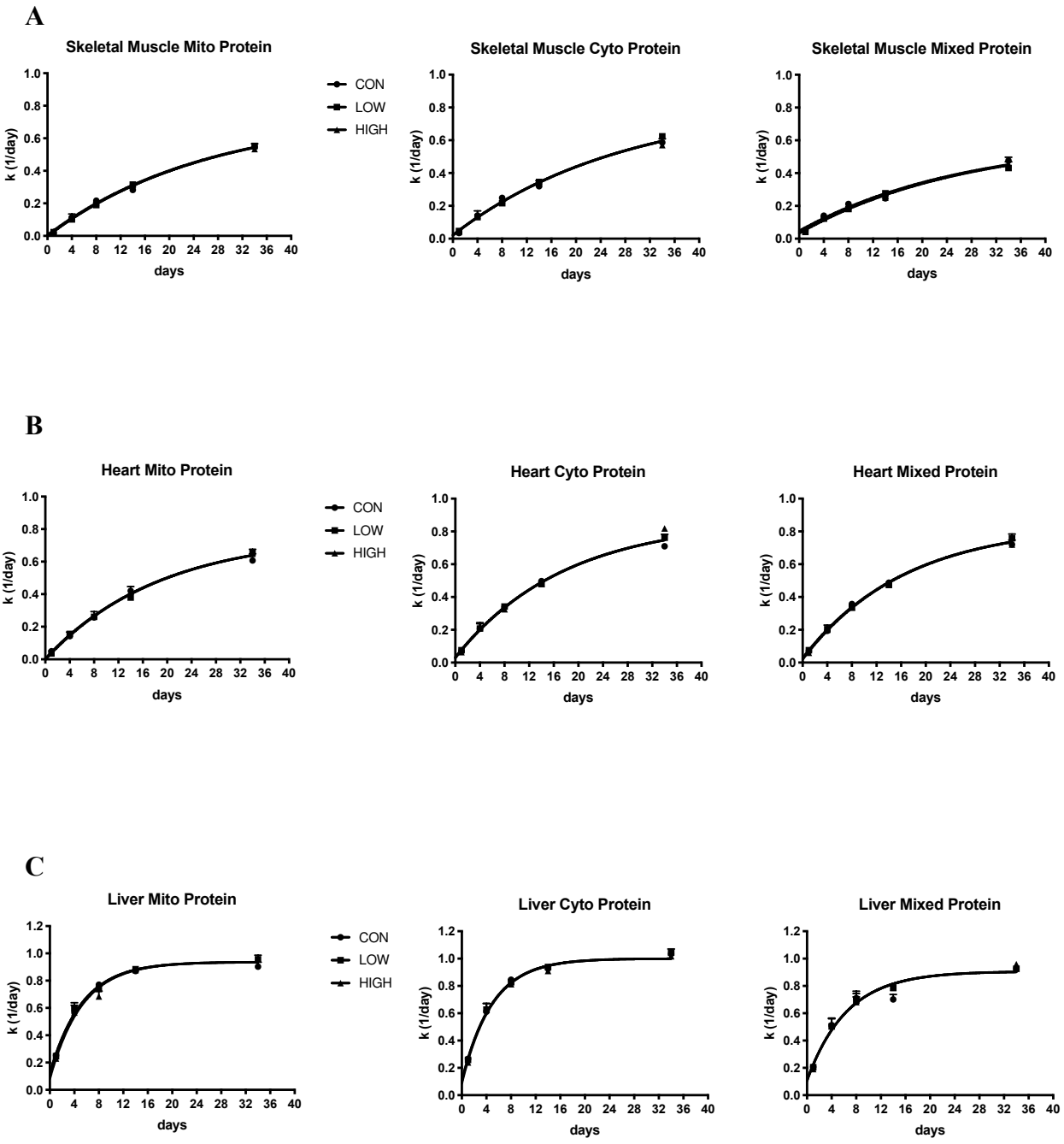

Figure 3. Protein fractional synthesis rates (FSR) in mito, cyto, and mixed subcellular fractions during 5 weeks of CON, LOW, or HIGH doses of PB125 supplementation in skeletal muscle (A), heart (B), and liver (C). Data are reported on 1, 4, 8, 14, and 34 days of deuterium labeling.

A

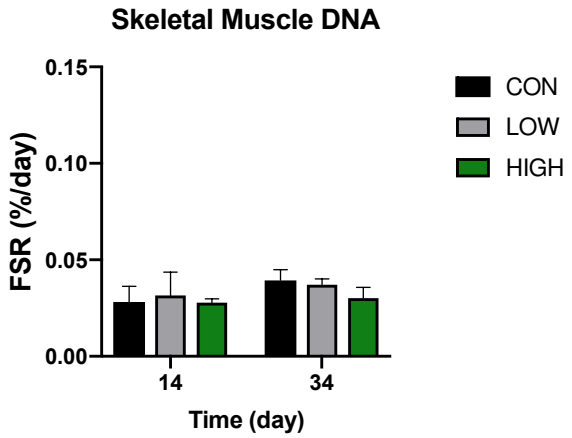

B

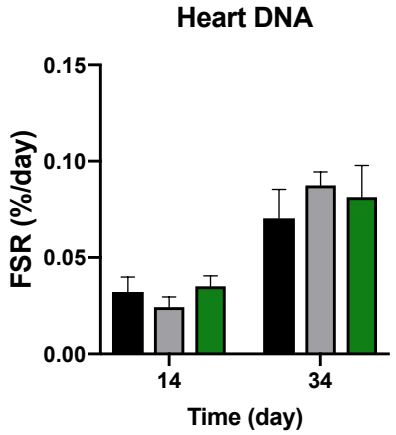

C

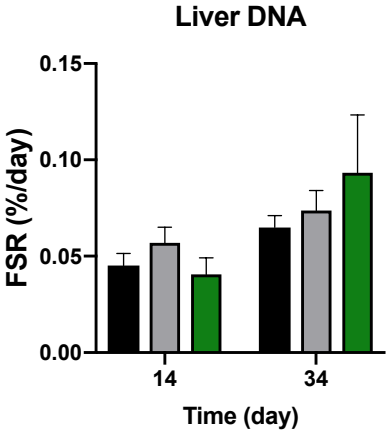

Figure 4. DNA fractional synthesis rates (FSR %/day) in skeletal muscle (A), heart (B), and liver (C) tissue after 14 and 34 days of deuterium labeling.

A

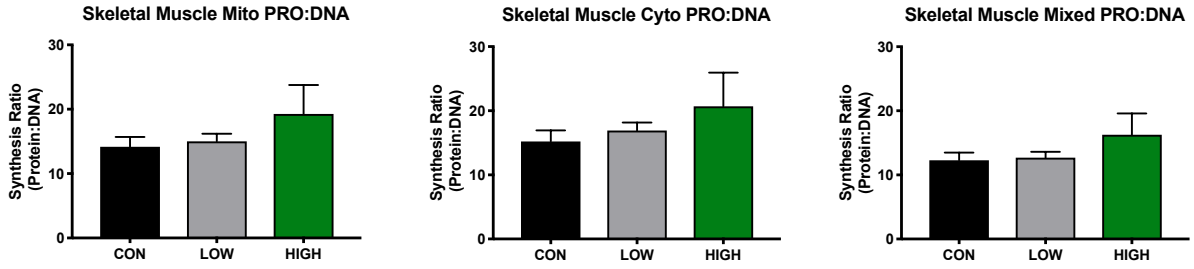

B

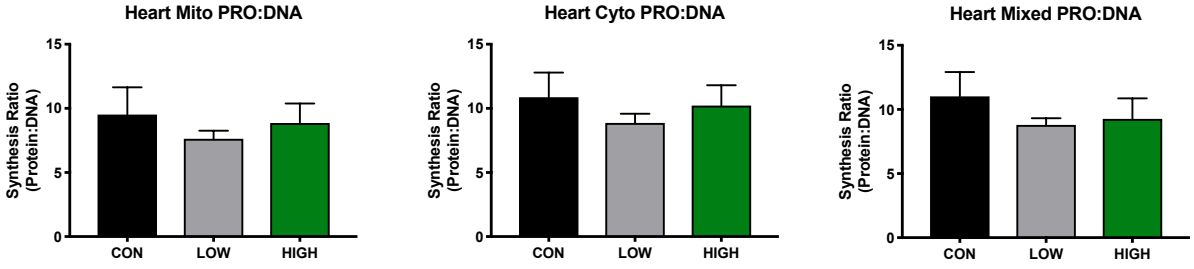

C

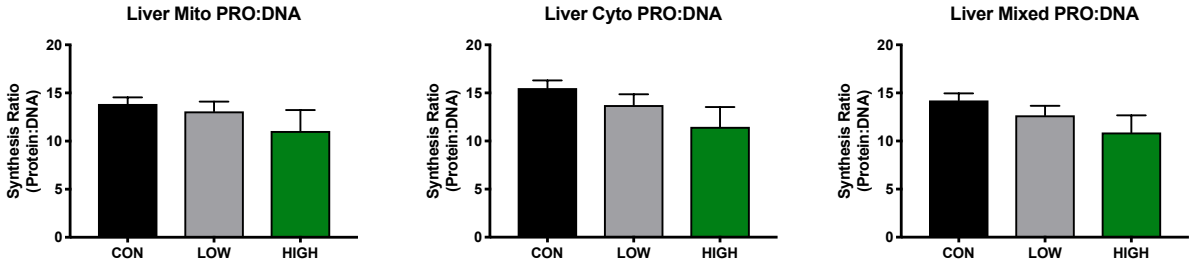

Figure 5. Synthetic ratios of PRO:DNA (FSR %/day) mito, cyto, and mixed subcellular fractions of skeletal muscle (A), heart (B), and liver (C) at two doses of PB125. Figures represent ratios at time point 34 days of deuterium labeling.

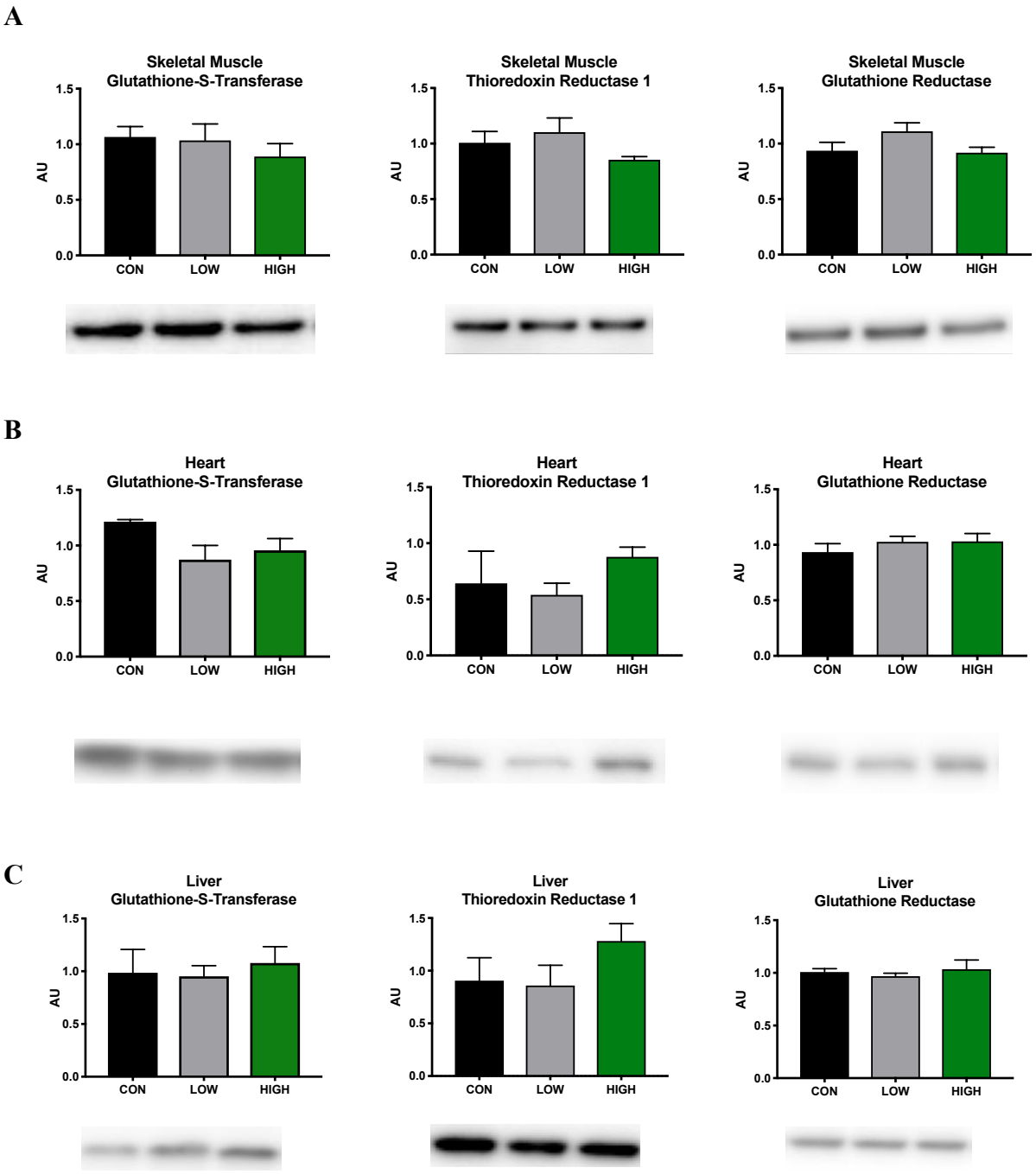

Figure 6. Content of antioxidant proteins Glutathione-S-Transferase (GST), Thioredoxin Reductase 1 (Trxr1), and Glutathione Reductase (GR) in skeletal muscle (A), heart (B), and liver (C). Reported data are from time point 34 (days) of deuterium labeling.

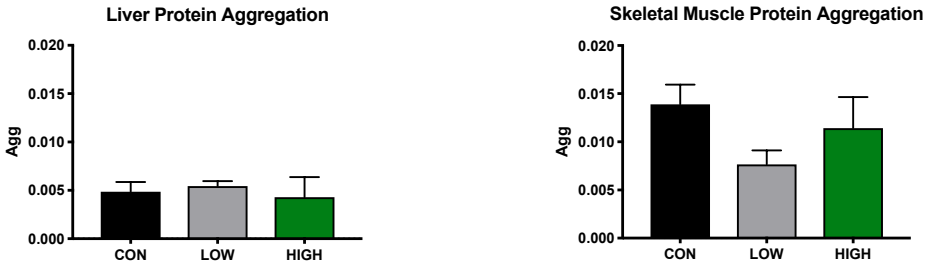

Figure 7. Quantification of protein aggregation in liver and skeletal muscle after 34 days of deuterium labeling.

I. Body Weight and Food Intake

There were no significant differences in body weight between treatment groups, however, all groups displayed a decrease in body weight pre to post 5-week feeding trial (Figure 2A). However, the weekly average body weight showed no statistical difference between each group over time. There were also no significant differences in average daily food intake between treatment groups (Figure 2B). Subjectively speaking, the mice tolerated both doses of PB125 supplemented diet, with no signs of gastrointestinal distress or abnormal behavior.

II. Protein and DNA Synthesis

Figure 3 demonstrates protein FSR (1/day) in skeletal muscle, heart, and liver tissue. There were no significant differences between treatment groups in protein FSR of mito, cyto, or mixed subcellular fractions of any tissue. To determine the influence of PB125 supplementation on mechanisms of proteostasis, protein:DNA (PRO:DNA) synthetic ratios (FSR %/day) were calculated for skeletal muscle, heart, and liver tissues at time

point 34 (days), which are displayed in Figure 5. Although there were no significant differences in PRO:DNA ratios, all tissues displayed similar trends between treatment groups in mito, cyto, and mixed fractions (Figure 5). Despite the lack of statistical significance, skeletal muscle (Figure 5A) had the highest PRO:DNA in the HIGH dose group, which may be partially explained by the insignificant trend toward reduced skeletal muscle DNA synthesis (Figure 4A). PRO:DNA ratios were not statistically different in heart and liver (Figure 5B-C). No significant differences were found in DNA FSR in any tissues (Figure 4A-C).

III. Protein Content and Aggregation

There were no significant differences in antioxidant protein content between PB125 treated groups in skeletal muscle, heart, or liver tissue at 34 days (Figure 6). To further investigate if PB125 improved mechanisms of proteostasis, we measured protein aggregation in skeletal muscle and liver tissue (Figure 7). There were no significant group differences.

CHAPTER V: DISCUSSION

I. Principal Outcomes

In the present study, protein and DNA synthesis rates were measured for the purpose of interrogating mechanisms of proteostatic maintenance in mitochondrial, cytosolic, and mixed subcellular fractions of skeletal muscle, heart, and liver tissue of 15-16 month old mice that were consuming a diet containing CON, LOW, or HIGH doses of the phytochemical Nrf2 activator PB125. We hypothesized that treatment with a PB125-supplemented diet (LOW and HIGH doses) would improve protein homeostasis, as indicated by an increased PRO:DNA synthesis ratio. Additionally, we hypothesized that mice consuming PB125 in their diet would have increased expression of antioxidant proteins and reduced levels of protein aggregation relative to the control group. Our findings show that protein and DNA synthesis rates in heart, liver, and skeletal muscle were unaffected by supplementation with PB125; and Nrf2-regulated protein expression of glutathione-S-transferase, thioredoxin reductase 1, and glutathione reductase were not significantly different between treatment groups in any tissues. Protein aggregation was measured in skeletal muscle and liver, with our results suggesting that PB125 supplementation did not affect protein aggregation. Collectively, we anticipated enhanced proteostasis outcomes in mice treated with either LOW or HIGH doses of PB125 compared to the control group. The principal outcome from this study is that protein homeostasis in PB125 treated mice is not statistically different than CON in subcellular fractions of skeletal muscle, heart or liver tissue.

II. Proteostasis

A key mechanism of protein homeostasis is the synthesis of new protein. As such, the primary goal of this study was to determine if treatment with the phytochemical-based Nrf2 activator, PB125, could improve proteostatic maintenance *in vivo*. To assess the role of PB125 in modulating proteostasis, the ratio of newly synthesized protein to DNA (PRO:DNA) was measured in skeletal muscle, heart, and liver tissue. Measuring rates of protein and DNA synthesis simultaneously facilitates evaluation of the contribution of cell proliferation to the measured rates of protein synthesis. Providing further context, a greater PRO:DNA ratio indicates that more of the protein synthetic resources are being allocated to repair and maintenance of existing cells (somatic maintenance) at the expense of cellular growth (proliferation). In agreement with this, our lab has previously demonstrated that targeting Nrf2 activation improves proteostasis during exposure to oxidative stress *in vitro*. Myoblasts co-cultured with the Nrf2 activator Protandim and H_2O_2 had improved mechanisms of proteostatic maintenance when faced with an oxidative challenge, as indicated by an increased PRO:DNA synthetic ratio (Bruns, Ehrlicher et al. 2018). Additionally, this study reports *in vivo* skeletal muscle data from rats treated with Protandim (600ppm) and allowed to run on exercise wheel for 6 weeks. Protandim was demonstrated to enhance mitochondrial proteostasis in the plantaris muscle, reflected by an increased PRO:DNA synthetic ratio only in the Protandim treated rats. However, in the present *in vivo* study using PB125, there were no significant differences in protein synthesis or in the accumulation of aggregated proteins, indicating that treatment with the Nrf2 activator had no apparent effect on *in vivo* proteostatic maintenance. Notably, the experimental design herein does not

support the detection of differences in PRO:DNA ratios at individual time points due to small sample sizes (n=3-4/group/timepoint). Rather, the experimental design was selected to determine long-term differences in synthesis rates of proteins with slow vs. rapid turnover, providing an advantageous approach to identify statistical differences in protein and DNA synthesis rates (k=1/day) over time. This data is generated by performing a one-phase non-linear curve fit using all time points throughout the five-week labeling period (Pettit, Jonsson et al. 2017). While we are not able to confirm the hypothesis that treatment with LOW and HIGH doses of PB125 results in increased PRO:DNA ratios relative to CON, a number of factors likely influenced our outcomes and require consideration upon interpreting our data; and as such, will be the focus of the forthcoming discussion.

Two primary factors may have limited our ability to detect differences in proteostatic maintenance and are, therefore, worthy of discussion. First, although the mice used were approaching old age, they were not otherwise “stressed.” Given that Nrf2 activation is indispensable for coordinating adaptive responses to oxidative and other stresses (Leung, Kwong et al. 2003), selecting a model subjected to stress might have revealed the true potential of PB125 to modulate proteostasis. Interrupting Nrf2 activity through genetic knockout offers a convenient model for understanding the biological consequences of dysfunctional Nrf2 signaling. Indeed, Nrf2 knockout severely affects the balance between ROS and antioxidants, causing increased incidence of pathology and cellular damage (Lee, Chan et al. 2004), and lethality during embryogenesis.

In the context of aging and disrupted Nrf2 activity, 24-month old mice were used in a study by Ahn and colleagues to investigate the role of Nrf2 deficiency on skeletal muscle quality and function. They found that Nrf2 deficient old mice have significantly decreased muscle mass and contractile dysfunction compared to their age-matched wild type counterparts (Ahn, Pharaoh et al. 2018). Another key parameter from this study is the measurement of mitochondrial function in permeabilized red gastrocnemius fibers of the old Nrf2 deficient mice, with results showing elevated ROS production, reduced complex I respiration, and an associated increase in the ratio of NAD^+ /NADH (Ahn, Pharaoh et al. 2018). In an independent study utilizing an aged Nrf2 knockout model, investigators revealed that the skeletal muscle of old mice lacking Nrf2 are deplete of antioxidants and GSH, which is associated with ROS accumulation and apoptosis. However, Nrf2 knockout in young animals did not affect antioxidant protein expression or ROS production, suggesting that the loss of Nrf2 in the absence of a stressed setting causes minimal disruptions to redox status (Miller, Gounder et al. 2012).

The necessity of Nrf2 activation was assessed in the presence and absence of stress by Li and colleagues by knocking out Nrf2 and evaluating cardiac function in response to hemodynamic stress. Nrf2 knockout did not result in any structural or functional changes to cardiac tissues in the absence of stress; however, when hemodynamic stress was induced by transverse aortic constriction there was significant myocardial fibrosis and apoptosis and increased levels of 4-HNE, a marker of oxidative damage (Li, Ichikawa et al. 2009). In contrast to Nrf2 knockout, several gain of function studies using

either phytochemical Nrf2 activation or Nrf2 overexpression have revealed that targeting Nrf2 activation confers stress resistance and cytoprotection (He, Kan et al. 2009, Liang, Li et al. 2017, Chen, Fan et al. 2019). Our group has confirmed this notion *in vitro* with human coronary artery endothelial cells. Specifically, these cells were treated with Protandim prior to an oxidative challenge and resulted in increased resistance to H_2O_2 compared to vehicle treated cells, and this resistance was indicated by significantly decreased nuclear apoptosis (Donovan, McCord et al. 2012). In a model using an adeno-associated virus to overexpress Nrf2, ROS levels were reduced *in vitro*, and *in vivo* mouse data with Nrf2 overexpression demonstrated a protective effect against acetaminophen-induced hepatotoxicity (Liang, Woodard et al. 2017). Furthermore, the available literature suggests that Nrf2 activation is indispensable for cellular function during aging and conditions of oxidative stress.

The second consideration that should be taken when interpreting our findings is the bioavailability of the active ingredients comprising PB125: carnosol, luteolin, and withaferin A. Briefly, these phytochemicals are metabolized in the intestines and liver into various metabolites. In this context, clarifying the concentration of metabolites as well as their distribution across tissues and organs is important for interpreting their biological effects *in vivo*. As such, a study conducted by Vaquero et al. employed oral administration of rosemary extract, the source of carnosol, to Zucker rats to assess metabolites and their respective concentrations in the small and large intestines, the liver, and plasma via LC-MS/MS analyses. Carnosol was rapidly detected in the intestines, liver, and plasma (Romo Vaquero, García Villalba et al. 2013). In a separate

study focused on characterizing the pharmokinetics of luteolin, Chen and colleagues used HPLC-MS to identify the concentration of luteolin in the plasma of rats and found that the plasma concentration of luteolin peaked 1 hour after oral administration, and was detectable for a total of 10 hours in the plasma (Chen, Liu et al. 2010). A recent study examining the bioavailability of luteolin determined that luteolin is efficiently absorbed in the intestine and then metabolized by the liver. However, luteolin is rapidly metabolized by enterocytes and hepatocytes into circulating metabolites, with luteolin-3'-O-ß-D-glucuronide being the most abundant metabolite across tissues. Thus, the resulting metabolites from oral luteolin administration contribute to its overall bioavailability (Deng, Gao et al. 2017). Lastly, it has been shown that withaferin A is detectable in the plasma of mice shortly after oral administration (Patil, Gautam et al. 2013). Though these investigations used higher doses of carnosol, luteolin, and withaferin A than the dosages in PB125, they provide useful insight to the absorption, distribution, metabolism, and excretion (ADME) of PB125's active ingredients. When taken collectively, the ADME data from these investigations indicate that carnosol, luteolin and withaferin A and their metabolic derivatives reach biologically relevant concentrations in the plasma and tissues when orally administered. However, the pharmokinetics of these compounds were not measured in the present study. Moreover, understanding the parameters surrounding the safety and bioavailability of PB125 allows for increased precision when developing phytochemical compounds and testing their applicability as therapeutic interventions.

III. Conclusions and Future Directions

To summarize, the present study is the first to characterize mechanisms of proteostatic maintenance following *o* treatment with PB125, a potent phytochemical Nrf2 activator, in 15-16-month-old C57BL6/J mice. The mice appeared to tolerate the PB125-supplemented diets well, providing further confirmation of PB125's safety when administered orally. The protein and DNA synthesis data do not confirm our group's previous studies showing that treatment with phytochemical Nrf2 activators cause marked improvements in proteostasis during an oxidative challenge. However, the use of an "unstressed" animal model in the present study may have limited our ability to detect significant differences in proteostasis outcomes. Future investigations are therefore necessary to discern whether treatment with PB125 can improve proteostasis *in vivo*. Preferably, future research would use experimental conditions that create robust impairments in protein homeostasis, such as in aged mice or an inducible model of stress in a specific tissue of interest. Additionally, future experiments should include both male and female animals, as data from the ITP suggest that the beneficial effects of phytochemical Nrf2 activation are sex specific, and this interaction is yet to be completely understood. For this reason, our group is currently examining the effects of long-term daily dosing with PB125 in both male and female Dunkin Hartley guinea pigs, an animal model utilized to study the progression of knee osteoarthritis and sarcopenia. Therefore, with careful consideration of our current findings and potential limitations discussed, future investigations will continue to focus on the potential of phytochemical Nrf2 activation as a promising therapeutic strategy for improving cellular function and extending healthspan.

REFERENCES

Ahn, B., G. Pharaoh, P. Premkumar, K. Huseman, R. Ranjit, M. Kinter, L. Szweda, T. Kiss, G. Fulop, S. Tarantini, A. Csiszar, Z. Ungvari and H. Van Remmen (2018). "Nrf2 deficiency exacerbates age-related contractile dysfunction and loss of skeletal muscle mass." Redox biology **17**: 47-58.

AnadÓN, A., M. R. MartÍNez-LarraÑAga, M. A. MartÍNez, I. Ares, M. R. GarcÍA-Risco, F. J. SeÑOrÁNs and G. Reglero (2008). "Acute Oral Safety Study of Rosemary Extracts in Rats." Journal of Food Protection **71**(4): 790-795.

Bakala, H., E. Delaval, M. Hamelin, J. Bismuth, C. Borot-Laloi, B. Corman and B. Friguet (2003). "Changes in rat liver mitochondria with aging." **270**(10): 2295-2302.

Basisty, N., J. G. Meyer and B. Schilling (2018). "Protein Turnover in Aging and Longevity." PROTEOMICS **18**(5-6): 1700108.

Beckman, K. B. and B. N. Ames (1998). "The Free Radical Theory of Aging Matures." Physiological Reviews **78**(2): 547-581.

Bellanti, F., A. D. Romano, A. Lo Buglio, V. Castriotta, G. Guglielmi, A. Greco, G. Serviddio and G. Vendemiale (2018). "Oxidative stress is increased in sarcopenia and associated with cardiovascular disease risk in sarcopenic obesity." Maturitas **109**: 6-12.

Bruns, D. R., S. E. Ehrlicher, S. Khademi, L. M. Biela, F. F. P. III, B. F. Miller and K. L. Hamilton (2018). "Differential effects of vitamin C or protandim on skeletal muscle adaptation to exercise." **125**(2): 661-671.

Cao, J., L. Li, C. Chen, C. Lv, F. Meng, L. Zeng, Z. Li, Q. Wu, K. Zhao, B. Pan, H. Cheng, W. Chen and K. Xu (2013). "RNA interference-mediated silencing of NANOG leads to reduced proliferation and self-renewal, cell cycle arrest and apoptosis in T-cell acute lymphoblastic leukemia cells via the p53 signaling pathway." **37**(9): 1170-1177.

Chandrasekhar, K., J. Kapoor and S. Anishetty (2012). "A prospective, randomized double-blind, placebo-controlled study of safety and efficacy of a high-concentration full-spectrum extract of ashwagandha root in reducing stress and anxiety in adults." Indian journal of psychological medicine **34**(3): 255-262.

Chen, R.-R., X.-H. Fan, G. Chen, G.-W. Zeng, Y.-G. Xue, X.-T. Liu and C.-Y. Wang (2019). "Irisin attenuates angiotensin II-induced cardiac fibrosis via Nrf2 mediated inhibition of ROS/ TGFβ1/Smad2/3 signaling axis." Chemico-Biological Interactions **302**: 11-21.

Chen, W., T. Jiang, H. Wang, S. Tao, A. Lau, D. Fang and D. D. Zhang (2012). "Does Nrf2 contribute to p53-mediated control of cell survival and death?" Antioxidants & redox signaling **17**(12): 1670-1675.

Chen, X., L. Liu, Z. Sun, Y. Liu, J. Xu, S. Liu, B. Huang, L. Ma, Z. Yu and K. Bi (2010). "Pharmacokinetics of luteolin and tetra-acetyl-luteolin assayed by HPLC in rats after oral administration." Biomedical Chromatography **24**(8): 826-832.

Chevet, E., C. Hetz and A. Samali (2015). "Endoplasmic Reticulum Stress–Activated Cell Reprogramming in Oncogenesis." Cancer Discovery **5**(6): 586.

Cullinan, S. B. and J. A. Diehl (2004). "PERK-dependent Activation of Nrf2 Contributes to Redox Homeostasis and Cell Survival following Endoplasmic Reticulum Stress." **279**(19): 20108-20117.

Cullinan, S. B. and J. A. Diehl (2006). "Coordination of ER and oxidative stress signaling: The PERK/Nrf2 signaling pathway." **38**(3): 317-332.

Cullinan, S. B., D. Zhang, M. Hannink, E. Arvisais, R. J. Kaufman and J. A. Diehl (2003). "Nrf2 Is a Direct PERK Substrate and Effector of PERK-Dependent Cell Survival." **23**(20): 7198-7209.

Dasarathy, S. and M. Hatzoglou (2018). "Hyperammonemia and proteostasis in cirrhosis." Current opinion in clinical nutrition and metabolic care **21**(1): 30-36.

Deng, C., C. Gao, X. Tian, B. Chao, F. Wang, Y. Zhang, J. Zou and D. Liu (2017). "Pharmacokinetics, tissue distribution and excretion of luteolin and its major metabolites in rats: Metabolites predominate in blood, tissues and are mainly excreted via bile." Journal of Functional Foods **35**: 332-340.

Diaz-Villanueva, J. F., R. Diaz-Molina and V. Garcia-Gonzalez (2015). "Protein Folding and Mechanisms of Proteostasis." Int J Mol Sci **16**(8): 17193-17230.

Dodson, M., M. R. de la Vega, A. B. Cholanians, C. J. Schmidlin, E. Chapman and D. D. Zhang (2019). "Modulating NRF2 in Disease: Timing Is Everything." Annual Review of Pharmacology and Toxicology **59**(1): 555-575.

Donato, A. J., I. Eskurza, A. E. Silver, A. S. Levy, G. L. Pierce, P. E. Gates and D. R. Seals (2007). "Direct Evidence of Endothelial Oxidative Stress With Aging in Humans: Relation to Impaired Endothelium-Dependent Dilation and Upregulation of Nuclear Factor- B." **100**(11): 1659-1666.

Donovan, E. L., J. M. McCord, D. J. Reuland, B. F. Miller and K. L. Hamilton (2012). "Phytochemical Activation of Nrf2 Protects Human Coronary Artery Endothelial Cells against an Oxidative Challenge." **2012**: 1-9.

Drake, J. C., D. R. Bruns, F. F. Peelor, 3rd, L. M. Biela, R. A. Miller, K. L. Hamilton and B. F. Miller (2014). "Long-lived crowded-litter mice have an age-dependent increase in

protein synthesis to DNA synthesis ratio and mTORC1 substrate phosphorylation." American journal of physiology. Endocrinology and metabolism **307**(9): E813-E821.

Egea, J., I. Fabregat, Y. M. Frapart, P. Ghezzi, A. Gorlach, T. Kietzmann, K. Kubaichuk, U. G. Knaus, M. G. Lopez, G. Olaso-Gonzalez, A. Petry, R. Schulz, J. Vina, P. Winyard, K. Abbas, O. S. Ademowo, C. B. Afonso, I. Andreadou, H. Antelmann, F. Antunes, M. Aslan, M. M. Bachschmid, R. M. Barbosa, V. Belousov, C. Berndt, D. Bernlohr, E. Bertran, A. Bindoli, S. P. Bottari, P. M. Brito, G. Carrara, A. I. Casas, A. Chatzi, N. Chondrogianni, M. Conrad, M. S. Cooke, J. G. Costa, A. Cuadrado, P. My-Chan Dang, B. De Smet, B. Debelec-Butuner, I. H. K. Dias, J. D. Dunn, A. J. Edson, M. El Assar, J. El-Benna, P. Ferdinandy, A. S. Fernandes, K. E. Fladmark, U. Forstermann, R. Giniatullin, Z. Giricz, A. Gorbe, H. Griffiths, V. Hampl, A. Hanf, J. Herget, P. Hernansanz-Agustin, M. Hillion, J. Huang, S. Ilikay, P. Jansen-Durr, V. Jaquet, J. A. Joles, B. Kalyanaraman, D. Kaminskyy, M. Karbaschi, M. Kleanthous, L. O. Klotz, B. Korac, K. S. Korkmaz, R. Koziel, D. Kracun, K. H. Krause, V. Kren, T. Krieg, J. Laranjinha, A. Lazou, H. Li, A. Martinez-Ruiz, R. Matsui, G. J. McBean, S. P. Meredith, J. Messens, V. Miguel, Y. Mikhed, I. Milisav, L. Milkovic, A. Miranda-Vizuete, M. Mojovic, M. Monsalve, P. A. Mouthuy, J. Mulvey, T. Munzel, V. Muzykantov, I. T. N. Nguyen, M. Oelze, N. G. Oliveira, C. M. Palmeira, N. Papaevgeniou, A. Pavicevic, B. Pedre, F. Peyrot, M. Phylactides, G. G. Pircalabioru, A. R. Pitt, H. E. Poulsen, I. Prieto, M. P. Rigobello, N. Robledinos-Anton, L. Rodriguez-Manas, A. P. Rolo, F. Rousset, T. Ruskovska, N. Saraiva, S. Sasson, K. Schroder, K. Semen, T. Seredenina, A. Shakirzyanova, G. L. Smith, T. Soldati, B. C. Sousa, C. M. Spickett, A. Stancic, M. J. Stasia, H. Steinbrenner, V. Stepanic, S. Steven, K. Tokatlidis, E. Tuncay, B. Turan, F. Ursini, J. Vacek, O. Vajnerova, K. Valentova, F. Van Breusegem, L. Varisli, E. A. Veal, A. S. Yalcin, O. Yelisyeyeva, N. Zarkovic, M. Zatloukalova, J. Zielonka, R. M. Touyz, A. Papapetropoulos, T. Grune, S. Lamas, H. Schmidt, F. Di Lisa and A. Daiber (2017). "European contribution to the study of ROS: A summary of the findings and prospects for the future from the COST action BM1203 (EU-ROS)." Redox Biol **13**: 94-162.
Enomoto, A. (2001). "High Sensitivity of Nrf2 Knockout Mice to Acetaminophen Hepatotoxicity Associated with Decreased Expression of ARE-Regulated Drug Metabolizing Enzymes and Antioxidant Genes." Toxicological Sciences **59**(1): 169-177.

Faraonio, R., P. Vergara, D. Di Marzo, M. G. Pierantoni, M. Napolitano, T. Russo and F. Cimino (2006). "p53 Suppresses the Nrf2-dependent Transcription of Antioxidant Response Genes." **281**(52): 39776-39784.

Fischer, N. W., A. Prodeus, D. Malkin and J. Gariépy (2016). "p53 oligomerization status modulates cell fate decisions between growth, arrest and apoptosis." Cell Cycle **15**(23): 3210-3219.

Freitas, I., E. Boncompagni, E. Tarantola, C. Gruppi, V. Bertone, A. Ferrigno, G. Milanesi, R. Vaccarone, M. E. Tira and M. Vairetti (2016). "In SituEvaluation of Oxidative Stress in Rat Fatty Liver Induced by a Methionine- and Choline-Deficient Diet." **2016**: 1-14.

Friedmann Angeli, J. P., M. Schneider, B. Proneth, Y. Y. Tyurina, V. A. Tyurin, V. J. Hammond, N. Herbach, M. Aichler, A. Walch, E. Eggenhofer, D. Basavarajappa, O. Rådmark, S. Kobayashi, T. Seibt, H. Beck, F. Neff, I. Esposito, R. Wanke, H. Förster, O. Yefremova, M. Heinrichmeyer, G. W. Bornkamm, E. K. Geissler, S. B. Thomas, B. R. Stockwell, V. B. O'Donnell, V. E. Kagan, J. A. Schick and M. Conrad (2014). "Inactivation of the ferroptosis regulator Gpx4 triggers acute renal failure in mice." Nature Cell Biology **16**(12): 1180-1191.

Gaikwad, A., D. J. Long, J. L. Stringer and A. K. Jaiswal (2001). "In Vivo Role of NAD(P)H:Quinone Oxidoreductase 1 (NQO1) in the Regulation of Intracellular Redox State and Accumulation of Abdominal Adipose Tissue." **276**(25): 22559-22564.
Giustarini, D., I. Dalle-Donne, D. Tsikas and R. Rossi (2009). "Oxidative stress and human diseases: Origin, link, measurement, mechanisms, and biomarkers." Crit Rev Clin Lab Sci **46**(5-6): 241-281.

Harding, H. P., I. Novoa, Y. Zhang, H. Zeng, R. Wek, M. Schapira and D. Ron (2000). "Regulated Translation Initiation Controls Stress-Induced Gene Expression in Mammalian Cells." Molecular Cell **6**(5): 1099-1108.

Harding, H. P., Y. Zhang, A. Bertolotti, H. Zeng and D. Ron (2000). "Perk Is Essential for Translational Regulation and Cell Survival during the Unfolded Protein Response." **5**(5): 897-904.

Harding, H. P., Y. Zhang and D. Ron (1999). "Protein translation and folding are coupled by an endoplasmic-reticulum-resident kinase." Nature **397**(6716): 271-274.
He, X., H. Kan, L. Cai and Q. Ma (2009). "Nrf2 is critical in defense against high glucose-induced oxidative damage in cardiomyocytes." Journal of Molecular and Cellular Cardiology **46**(1): 47-58.

Hiemstra, S., M. Niemeijer, E. Koedoot, S. Wink, J. E. Klip, M. Vlasveld, E. de Zeeuw, B. van Os, A. White and B. v. d. Water (2017). "Comprehensive Landscape of Nrf2 and p53 Pathway Activation Dynamics by Oxidative Stress and DNA Damage." Chemical Research in Toxicology **30**(4): 923-933.

Itoh, K., T. Chiba, S. Takahashi, T. Ishii, K. Igarashi, Y. Katoh, T. Oyake, N. Hayashi, K. Satoh, I. Hatayama, M. Yamamoto and Y.-I. Nabeshima (1997). "An Nrf2/Small Maf Heterodimer Mediates the Induction of Phase II Detoxifying Enzyme Genes through Antioxidant Response Elements." Biochemical and Biophysical Research Communications **236**(2): 313-322.

Itoh, K., N. Wakabayashi, Y. Katoh, T. Ishii, K. Igarashi, J. D. Engel and M. Yamamoto (1999). "Keap1 represses nuclear activation of antioxidant responsive elements by Nrf2 through binding to the amino-terminal Neh2 domain." Genes & development **13**(1): 76-86.

Jain, A., T. Lamark, E. Sjottem, K. Bowitz Larsen, J. Atesoh Awuh, A. Overvatn, M. McMahon, J. D. Hayes and T. Johansen (2010). "p62/SQSTM1 Is a Target Gene for Transcription Factor NRF2 and Creates a Positive Feedback Loop by Inducing Antioxidant Response Element-driven Gene Transcription." **285**(29): 22576-22591.

Jang, J., Y. Wang, H.-S. Kim, M. A. Lalli and K. S. Kosik (2014). "Nrf2, a regulator of the proteasome, controls self-renewal and pluripotency in human embryonic stem cells." Stem cells (Dayton, Ohio) **32**(10): 2616-2625.

Johnson, J. J. (2011). "Carnosol: a promising anti-cancer and anti-inflammatory agent." Cancer letters **305**(1): 1-7.

Klaips, C. L., G. G. Jayaraj and F. U. Hartl (2018). "Pathways of cellular proteostasis in aging and disease." J Cell Biol **217**(1): 51-63.

Kohno, K., K. Normington, J. Sambrook, M. J. Gething and K. Mori (1993). "The promoter region of the yeast KAR2 (BiP) gene contains a regulatory domain that responds to the presence of unfolded proteins in the endoplasmic reticulum." Molecular and cellular biology **13**(2): 877-890.

Komatsu, M., H. Kurokawa, S. Waguri, K. Taguchi, A. Kobayashi, Y. Ichimura, Y.-S. Sou, I. Ueno, A. Sakamoto, K. I. Tong, M. Kim, Y. Nishito, S.-I. Iemura, T. Natsume, T. Ueno, E. Kominami, H. Motohashi, K. Tanaka and M. Yamamoto (2010). "The selective autophagy substrate p62 activates the stress responsive transcription factor Nrf2 through inactivation of Keap1." Nature Cell Biology **12**(3): 213-223.

Kwak, M.-K., N. Wakabayashi, J. L. Greenlaw, M. Yamamoto and T. W. Kensler (2003). "Antioxidants enhance mammalian proteasome expression through the Keap1-Nrf2 signaling pathway." Molecular and cellular biology **23**(23): 8786-8794.

Lee, J. M., K. Chan, Y. W. Kan and J. A. Johnson (2004). "Targeted disruption of Nrf2 causes regenerative immune-mediated hemolytic anemia." **101**(26): 9751-9756.

Leung, L., M. Kwong, S. Hou, C. Lee and J. Y. Chan (2003). "Deficiency of the Nrf1 and Nrf2 Transcription Factors Results in Early Embryonic Lethality and Severe Oxidative Stress." **278**(48): 48021-48029.

Lewis, K. N., J. Mele, J. D. Hayes and R. Buffenstein (2010). "Nrf2, a Guardian of Healthspan and Gatekeeper of Species Longevity." **50**(5): 829-843.

Li, J., T. Ichikawa, L. Villacorta, J. S. Janicki, G. L. Brower, M. Yamamoto and T. Cui (2009). "Nrf2 Protects Against Maladaptive Cardiac Responses to Hemodynamic Stress." **29**(11): 1843-1850.

Liang, J., L. Li, Y. Sun, W. He, X. Wang and Q. Su (2017). "The protective effect of activating Nrf2 / HO-1 signaling pathway on cardiomyocyte apoptosis after coronary microembolization in rats." BMC Cardiovascular Disorders **17**(1): 272.

Liang, K. J., K. T. Woodard, M. A. Weaver, J. P. Gaylor, E. R. Weiss and R. J. Samulski (2017). "AAV- Nrf2 Promotes Protection and Recovery in Animal Models of Oxidative Stress." **25**(3): 765-779.

Lim, J., M. L. Lachenmayer, S. Wu, W. Liu, M. Kundu, R. Wang, M. Komatsu, Y. J. Oh, Y. Zhao and Z. Yue (2015). "Proteotoxic stress induces phosphorylation of p62/SQSTM1 by ULK1 to regulate selective autophagic clearance of protein aggregates." PLoS genetics **11**(2): e1004987-e1004987.

Liu, W. J., L. Ye, W. F. Huang, L. J. Guo, Z. G. Xu, H. L. Wu, C. Yang and H. F. Liu (2016). "p62 links the autophagy pathway and the ubiqutin-proteasome system upon ubiquitinated protein degradation." Cellular & molecular biology letters **21**: 29-29.

Luo, H., H. Liang, J. Chen, Y. Xu, Y. Chen, L. Xu, L. Yun, J. Liu, H. Yang, L. Liu, J. Peng, Z. Liu, L. Tang, W. Chen and H. Tang (2017). "Hydroquinone induces TK6 cell growth arrest and apoptosis through PARP-1/p53 regulatory pathway." Environmental Toxicology.

MacLeod, A. K., M. McMahon, S. M. Plummer, L. G. Higgins, T. M. Penning, K. Igarashi and J. D. Hayes (2009). "Characterization of the cancer chemopreventive NRF2-dependent gene battery in human keratinocytes: demonstration that the KEAP1-NRF2 pathway, and not the BACH1-NRF2 pathway, controls cytoprotection against electrophiles as well as redox-cycling compounds." Carcinogenesis **30**(9): 1571-1580.

Malumbres, M. (2014). "Cyclin-dependent kinases." **15**(6): 122.

Márton, M., N. Tihanyi, P. Gyulavári, G. Bánhegyi and O. Kapuy (2018). "NRF2-regulated cell cycle arrest at early stage of oxidative stress response mechanism." PloS one **13**(11): e0207949-e0207949.

McCord, J. M. and I. Fridovich (1968). "The Reduction of Cytochrome c by Milk Xanthine Oxidase." Journal of Biological Chemistry **243**(21): 5753-5760.

McLendon, P. M. and J. Robbins (2015). "Proteotoxicity and cardiac dysfunction." Circ Res **116**(11): 1863-1882.

Meng, S.-J. and L.-J. Yu (2010). "Oxidative stress, molecular inflammation and sarcopenia." International journal of molecular sciences **11**(4): 1509-1526.

Miller, B. F., M. M. Robinson, M. D. Bruss, M. Hellerstein and K. L. Hamilton (2012). "A comprehensive assessment of mitochondrial protein synthesis and cellular proliferation with age and caloric restriction." Aging Cell **11**(1): 150-161.

Miller, B. F., M. M. Robinson, D. J. Reuland, J. C. Drake, F. F. Peelor, 3rd, M. D. Bruss, M. K. Hellerstein and K. L. Hamilton (2013). "Calorie restriction does not increase short-term or long-term protein synthesis." J Gerontol A Biol Sci Med Sci **68**(5): 530-538.

Miller, C. J., S. S. Gounder, S. Kannan, K. Goutam, V. R. Muthusamy, M. A. Firpo, J. D. Symons, R. Paine, J. R. Hoidal and N. S. Rajasekaran (2012). "Disruption of Nrf2/ARE signaling impairs antioxidant mechanisms and promotes cell degradation pathways in aged skeletal muscle." **1822**(6): 1038-1050.

Murali, G. and C. Panneerselvam (2007). Age-Associated Oxidative Macromolecular Damages in Rat Brain Regions: Role of Glutathione Monoester.

Nguyen, T., P. Nioi and C. B. Pickett (2009). "The Nrf2-antioxidant response element signaling pathway and its activation by oxidative stress." The Journal of biological chemistry **284**(20): 13291-13295.

Nishimoto, S., S. Koike, N. Inoue, T. Suzuki and Y. Ogasawara (2017). "Activation of Nrf2 attenuates carbonyl stress induced by methylglyoxal in human neuroblastoma cells: Increase in GSH levels is a critical event for the detoxification mechanism."
Noda, N. N. and F. Inagaki (2015). "Mechanisms of Autophagy." **44**(1): 101-122.

Okoduwa, S. I., I. A. Umar, S. Ibrahim, F. Bello and N. Habila (2015). "Age-dependent alteration of antioxidant defense system in hypertensive and type-2 diabetes patients." Journal of diabetes and metabolic disorders **14**: 32-32.

Pajares, M., N. Jiménez-Moreno, Á. J. García-Yagüe, M. Escoll, M. L. De Ceballos, F. Van Leuven, A. Rábano, M. Yamamoto, A. I. Rojo and A. Cuadrado (2016). "Transcription factor NFE2L2/NRF2 is a regulator of macroautophagy genes." **12**(10): 1902-1916.

Patil, D., M. Gautam, S. Mishra, S. Karupothula, S. Gairola, S. Jadhav, S. Pawar and B. Patwardhan (2013). "Determination of withaferin A and withanolide A in mice plasma using high-performance liquid chromatography-tandem mass spectrometry: Application to pharmacokinetics after oral administration of Withania somnifera aqueous extract." **80**: 203-212.

Pettit, A. P., W. O. Jonsson, A. R. Bargoud, E. T. Mirek, F. F. Peelor, 3rd, Y. Wang, T. W. Gettys, S. R. Kimball, B. F. Miller, K. L. Hamilton, R. C. Wek and T. G. Anthony (2017). "Dietary Methionine Restriction Regulates Liver Protein Synthesis and Gene Expression Independently of Eukaryotic Initiation Factor 2 Phosphorylation in Mice." The Journal of nutrition **147**(6): 1031-1040.

Reuland, D. J., S. Khademi, C. J. Castle, D. C. Irwin, J. M. McCord, B. F. Miller and K. L. Hamilton (2013). "Upregulation of phase II enzymes through phytochemical activation of Nrf2 protects cardiomyocytes against oxidant stress." Free Radic Biol Med **56**: 102-111.

Reynaert, N. L., P. Gopal, E. P. A. Rutten, E. F. M. Wouters and C. G. Schalkwijk (2016). "Advanced glycation end products and their receptor in age-related, non-communicable chronic inflammatory diseases; Overview of clinical evidence and potential contributions to disease."

Richardson, A. G. and E. E. Schadt (2014). "The Role of Macromolecular Damage in Aging and Age-related Disease." The Journals of Gerontology: Series A **69**(Suppl_1): S28-S32.

Richter-Dennerlein, R., S. Oeljeklaus, I. Lorenzi, C. Ronsor, B. Bareth, A. B. Schendzielorz, C. Wang, B. Warscheid, P. Rehling and S. Dennerlein (2016). "Mitochondrial Protein Synthesis Adapts to Influx of Nuclear-Encoded Protein." Cell **167**(2): 471-483 e410.

Romo Vaquero, M., R. García Villalba, M. Larrosa, M. J. Yáñez-Gascón, E. Fromentin, J. Flanagan, M. Roller, F. A. Tomás-Barberán, J. C. Espín and M.-T. García-Conesa (2013). "Bioavailability of the major bioactive diterpenoids in a rosemary extract: Metabolic profile in the intestine, liver, plasma, and brain of Zucker rats." Molecular Nutrition & Food Research **57**(10): 1834-1846.

Ron, D. and P. Walter (2007). "Signal integration in the endoplasmic reticulum unfolded protein response." Nature Reviews Molecular Cell Biology **8**(7): 519-529.

Ryazanov, A. G. and B. S. Nefsky (2002). "Protein turnover plays a key role in aging." **123**(2-3): 207-213.

Seals, D. R., K. L. Jablonski and A. J. Donato (2011). "Aging and vascular endothelial function in humans." Clin Sci (Lond) **120**(9): 357-375.

Strong, R., R. A. Miller, A. Antebi, C. M. Astle, M. Bogue, M. S. Denzel, E. Fernandez, K. Flurkey, K. L. Hamilton, D. W. Lamming, M. A. Javors, J. P. de Magalhaes, P. A. Martinez, J. M. McCord, B. F. Miller, M. Muller, J. F. Nelson, J. Ndukum, G. E. Rainger, A. Richardson, D. M. Sabatini, A. B. Salmon, J. W. Simpkins, W. T. Steegenga, N. L. Nadon and D. E. Harrison (2016). "Longer lifespan in male mice treated with a weakly estrogenic agonist, an antioxidant, an alpha-glucosidase inhibitor or a Nrf2-inducer." Aging Cell **15**(5): 872-884.

Tebay, L. E., H. Robertson, S. T. Durant, S. R. Vitale, T. M. Penning, A. T. Dinkova-Kostova and J. D. Hayes (2015). "Mechanisms of activation of the transcription factor Nrf2 by redox stressors, nutrient cues, and energy status and the pathways through which it attenuates degenerative disease." **88**: 108-146.

Valko, M., D. Leibfritz, J. Moncol, M. T. D. Cronin, M. Mazur and J. Telser (2007). "Free radicals and antioxidants in normal physiological functions and human disease." The International Journal of Biochemistry & Cell Biology **39**(1): 44-84.

Wild, A. C., H. R. Moinova and R. T. Mulcahy (1999). "Regulation of -Glutamylcysteine Synthetase Subunit Gene Expression by the Transcription Factor Nrf2." **274**(47): 33627-33636.

Wong, H. S., P. A. Dighe, V. Mezera, P. A. Monternier and M. D. Brand (2017). "Production of superoxide and hydrogen peroxide from specific mitochondrial sites under different bioenergetic conditions." J Biol Chem **292**(41): 16804-16809.

Wu, K. C., J. Y. Cui and C. D. Klaassen (2012). "Effect of Graded Nrf2 Activation on Phase-I and -II Drug Metabolizing Enzymes and Transporters in Mouse Liver." **7**(7): e39006.

Wu, K. C., P. R. McDonald, J. Liu and C. D. Klaassen (2014). "Screening of natural compounds as activators of the keap1-nrf2 pathway." Planta Med **80**(1): 97-104.

Xie, W., M. Pariollaud, W. E. Wixted, N. Chitnis, J. Fornwald, M. Truong, C. Pao, Y. Liu, R. S. Ames, J. Callahan, R. Solari, Y. Sanchez, A. Diehl and H. Li (2015). "Identification and Characterization of PERK Activators by Phenotypic Screening and Their Effects on NRF2 Activation." **10**(3): e0119738.

Yamada, M., M. Iwata, E. Warabi, H. Oishi, V. A. Lira and M. Okutsu (2019). "p62/SQSTM1 and Nrf2 are essential for exercise-mediated enhancement of antioxidant protein expression in oxidative muscle." The FASEB Journal: fj.201900133R.

Zhang, D. D., S. C. Lo, J. V. Cross, D. J. Templeton and M. Hannink (2004). "Keap1 is a redox-regulated substrate adaptor protein for a Cul3-dependent ubiquitin ligase complex." Mol Cell Biol **24**(24): 10941-10953.

Zhou, L., H. Zhang, K. J. A. Davies and H. J. Forman (2018). "Aging-related decline in the induction of Nrf2-regulated antioxidant genes in human bronchial epithelial cells." Redox Biology **14**: 35-40.